"Oxidation of New Materials and Composites" (manuscript code ONMC-4)

Enhanced Oxidation Resistance of Mo-Si-B-Ti Alloys By Pack-Cementation

Daniel Schliephake[a], Camelia Gombola[a], Alexander Kauffmann[a], Martin Heilmaier[a], John H. Perepezko[b]

[a]*Karlsruhe Institute of Technology (KIT), Institute for Applied Materials, Engelbert-Arnold-Str. 4, 76131 Karlsruhe, GERMANY*
[b]*University of Wisconsin – Madison, Department of Materials Science and Engineering, 1509 University Avenue, Madison, WI 53706, USA*

daniel.schliephake@kit.edu; camelia.gombola@kit.edu; alexander.kauffmann@kit.edu; martin.heilmaier@kit.edu; perepezk@engr.wisc.edu

Abstract.
As new high temperature structural materials, Mo-Si-B alloys satisfy several requirements such as oxidation and creep resistance. Recently, novel Ti-rich Mo-Si-B alloys have shown an increased creep resistance compared to Ti-free alloys. However, due to the formation of a duplex SiO_2 – TiO_2 oxide layer, which allows for fast ingress of oxygen, the oxidation resistance is poor. To improve the oxidation resistance a borosilicate based coating was applied to a Mo-12.5Si-8.5B-27.5Ti (in at.%) alloy. After co-deposition of Si and B by pack cementation at 1000 °C in Ar, a conditioning anneal at 1400 °C is used to develop an outer borosilicate layer followed by an inner $MoSi_2$ and Mo_5Si_3 layer. During both isothermal and cyclic oxidation after an initial mass loss during the first hours of exposure, a steady state is reached for times up to 1000 h at temperatures ranging from 800 to 1200 °C demonstrating a significantly enhanced oxidation resistance.

Keywords: High-temperature Materials, Mo-Si-B-Ti Alloys, Pack-cementation, Oxidation Resistant Coating

INTRODUCTION

New high-temperature structural materials are required to deal with the challenges in power generation and air transportation. To increase the efficiency of power generation and aircraft engines, a higher combustion temperature is one possible solution. To withstand the additional oxidation and creep demands, materials with higher melting points like Nb- or Mo-silicide alloys are promising candidates [1 – 3]. Because of their good creep and oxidation behavior at 1200 °C, multiphase Mo_{ss} + Mo_5SiB_2 + Mo_3Si alloys have attracted a growing interest for the last two decades [4 – 7]. Unfortunately, such alloys exhibit a relatively high density of 9.6 g/cm³ compared to densities below 9 g/cm³ for common Ni-base superalloys [8] and fail in a brittle manner at lower temperatures [9 – 12]. Furthermore, at temperatures at around 600 – 900 °C the oxidation resistance of Mo-Si-B alloys is dominated by MoO_3 vaporization and results in a catastrophic oxidation behavior [13].

Recently, novel Ti-rich Mo_{ss} + Mo_5SiB_2 + Mo_3Si alloys have shown an increased creep resistance and lowered density of 7.8 g/cm³ compared to Ti-free Mo-Si-B alloys [14], [15]. The enhanced creep resistance is due to the formation of Ti-silicide precipitates within the Mo solid solution phase (Mo_{ss}) during processing. However, these alloys exhibit poor oxidation resistance, due to the formation of a duplex SiO_2 – TiO_2 surface layer that allows for fast inward diffusion of oxygen [16]. This leads to a catastrophic oxidation at 820 and 1000 °C and to an almost linear mass loss at 1100 °C and above. Furthermore, Yang et al. [17] found that alloying with Ti can stabilize the Mo_5Si_3 phase in exchange for Mo_3Si. As first reported by Burk et al. the Ti-rich Mo_5Si_3 phase shows an increased oxidation resistance compared to the Ti-free phase and Mo_3Si. [18]. Since the Mo_5Si_3 phase is difficult to stabilize under the conditions described by Yang et al. [17], Fe as further minor alloying element was added by

Azim et al. [15] to enlarge the Mo_{ss} + Mo_5SiB_2 + Mo_5Si_3 phase field. Nevertheless, even by stabilizing a multiphase Mo_{ss} + Mo_5SiB_2 + Mo_5Si_3 microstructure the oxidation resistance is still small compared to Ni-based superalloys [19].

For structural applications the requirements for high strength at high temperature along with environmental attack resistance are not usually satisfied concurrently for most materials. One effective strategy to address an enhanced resistance to environmental attack in high- strength materials is the application of oxidation-resistant coatings. While this strategy is attractive, the successful implementation of protective coatings over the entire operating temperature range need the satisfaction of other requirements involving thermodynamic and mechanical compatibility between the coating and the alloy substrate and the robust stability of the coating in order to maintain the integrity of the environmental protection. For further improvement in oxidation resistance a pre-treatment of the surface is inevitable to preserve the excellent creep behavior and low density of Ti-rich Mo-Si-B alloys. In the past, different coating systems were applied on Mo-Si-B alloys. To deposit an Al-containing coating Sakidja et al. [20] used the Al-pack cementation process which was already established for Ni-base superalloys. After subsequent annealing in air, the coated samples were protected against further oxidation by an outer Al_2O_3 layer at all tested temperatures ranging from 732 to 1372 °C. Additionally, the coating consists of two more inner layers, (i) a mixture of Mo_3Al_8 and Mo_3Si and of (ii) Mo_3Si and Mo_5SiB_2. Park et al. [21] covered Mo-Si-B alloys by a SiO_2/ethanol slurry using an air gun followed by annealing at 1000 or 1200°C in air. After annealing the coating consists of three separate layers: (i) an exterior borosilicate glass layer, (ii) a mixed glass and MoO_2 layer and (iii) the Mo_{ss} phase. Sakidja et al. [22] designed silicide-based coatings by (Si+B)-pack cementation, which also resulted in a three layer arrangement after exposure in air: (i) an outer borosilicate layer, (ii) a B saturated Mo_5Si_3 layer and (iii) a Mo_5SiB_2 layer. Both, Park and Sakidja found an enhanced oxidation resistance of their coated alloys compared to uncoated samples at temperatures ranging from 1000 to 1300 °C.

To enhance the oxidation resistance of Ti-rich Mo-Si-B alloys, the present work examined the effectiveness of (Si+B)-pack cementation on a model Mo-12.5Si-8.5B-27.5Ti alloy. The reaction of the coating with the substrate during processing and with the oxidizing atmosphere were determined as a function of temperature and time. Both, isothermal and cyclic oxidation exposures have been carried out at temperatures ranging from 800 to 1200 °C.

EXPERIMENTAL PROCEDURES

The Mo-12.5Si-8.5B-27.5Ti (in at.%) substrate material was produced by repetitive arc-melting of high-purity metals, Si and B in a Zr gettered high-purity Ar-atmosphere. After homogenization treatment at 1600 °C for 100 h slices of this alloy were prepared for pack-cementation. The substrate slices with a thickness of 4.5 mm were embedded in a powder mixture consisting of 62.5 wt.% Al_2O_3, 35 wt.% Si + B and 2.5 wt.% NaF. Subsequently, the pack-cementation was carried out in an Ar-atmosphere at 1000°C for 40h to co-deposit the Si and B. Finally, the conditioning takes place at 1400 °C for 10h in air. A detailed description of the pack-cementation process can be found elsewhere [22], [23].

The oxidation behavior was studied under isothermal conditions by continuous thermogravimetric analysis (TGA) and under thermal cycling conditions by measuring the weight change. TGA was carried out in synthetic air (80% O_2, 20% N_2) at 1100 and 1200 °C with a flow rate of 30 ml/min using a Netzsch STA449 F1 Jupiter on single samples. The thermal cycling oxidation experiments were carried out in a box-type furnace at 800°C up to 1000 h and at 1100 and 1200 °C up to 500 h in ambient air to study the long term oxidation behavior using three different samples for each temperature. The exposure times were 1 h at the beginning of the cycling and were increased to 5, 20, 50 and 100 h cycles during advanced oxidation. After half of the maximum exposure times the cyclic oxidation tests were stopped for one of the samples to analyze the microstructure and oxidation products by scanning electron microscopy (SEM) and electron-backscattered diffraction (EBSD). For both, isothermal and thermal cycling oxidation all samples were held in alumina crucibles.

TABLE 1. List of oxidation tests

Temperature in °C	Oxidation mode	Time Sample A in h	Time Sample B in h	Time Sample C in h
800	Thermal Cycling	500	1000	1000
1100	Isothermal	100	100	
	Thermal Cycling	250	500	500
1200	Isothermal	100	100	
	Thermal Cycling	250	500	500

SEM examination was carried out in secondary-electron (SE) and backscattered-electron (BSE) mode using a Zeiss EVO50 microscopy. The relevant elements as well as their distribution were determined qualitatively by energy-dispersive X- ray spectroscopy (EDS). To confirm thermal stability of the substrate microstructure the phase distribution was determined using an image processing program. A Zeiss Auriga 60 SEM equipped with an EDAX System for EDS and EBSD was used to determine the local crystal-structure of the layer-composition after pack-cementation and the resulting oxidation products. Electron beam microanalysis (EPMA) with a Cameca SX51 instrument (8 kV, 20 na) was used for detection of boron in the coating.

RESULTS AND DISCUSSION

Microstructure and layer arrangement after conditioning

A representative microstructure of the substrate alloy with the pack cementation coating after conditioning at 1400 °C for 10 h is shown in Fig. 1. The substrate microstructure is nearly the same as reported in a previous work on Mo-Si-B-Ti alloys [14] and consists of Mo_{ss}, Mo_3Si, Mo_5SiB_2 and Ti_5Si_3. Table 2 summarizes the present phases and their calculated volume fractions using an image processing program for the substrate material at all processing steps and at all oxidation temperatures with 500 h of exposure time. During the conditioning at 1400 °C the phase distribution changes significantly for Mo_{ss}, Mo_3Si and Ti_5Si_3, due to the eutectoid reaction of $Mo_3Si \leftrightarrow Mo_{ss} + Ti_5Si_3$ found by Azim et al. [15]. The volume fraction of Mo_3Si decreases from 29.8 to 6.7 Vol.% after 10 h at 1400 °C. Since this eutectoid reaction is diffusion controlled, 10 h at 1400 °C will not lead to completion of the transformation because of the low diffusivity in Mo-Si-B alloys [25 – 27]. Nevertheless, after 500 h at 1200 °C no evidence of Mo_3Si was found, while at 800 and 1100 °C, residual Mo_3Si is still present.

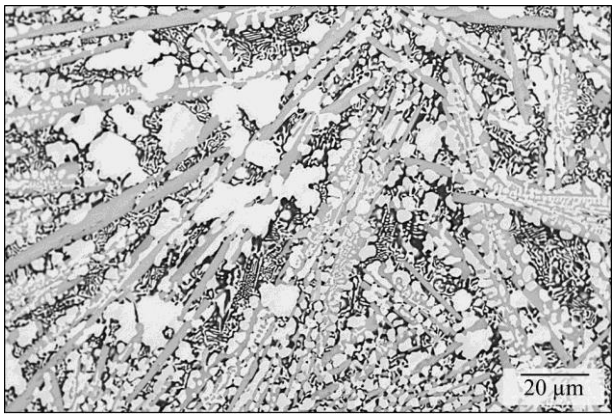

FIG. 1. SEM micrograph showing substrate material after conditioning at 1400 °C for 10 h

TABLE 2. Phase distribution (Vol%) in substrate for different exposure times and temperatures

Phase	Homogenization 1600 °C/100 h	Conditioned 1400 °C/10 h	Oxidation 800 °C/500 h	Oxidation 1100 °C/500 h	Oxidation 1200 °C/500 h
Mo_{ss}	32.09 (±1.1)	39.70 (±2.2)	43.77 (±2.1)	45.30 (±3.0)	44.35 (±1.6)
Mo_5SiB_2	33.45 (±0.8)	34.14 (±3.1)	37.15 (±2.4)	33.27 (±3.1)	37.48 (±1.6)
Ti_5Si_3	4.57 (±0.5)	19.13 (±1.9)	17.18 (±3.7)	20.67 (±3.7)	18.17 (±1.3)
Mo_3Si	29.88 (±0.9)	6.77 (±2.3)	1.66 (±1.6)	1.04 (±0.78)	-

Fig. 2 a) shows the residual layer after the pack cementation process consists of $MoSi_2$, where different Ti-contents results in a slightly different BSE contrast. After conditioning at 1400 °C for 10 h the coating consists of three separate layers as shown in Fig. 2 b). The outer layer consists of borosilicate which is consistent with observations in literature on (Si+B) pack cementation of Mo-Si-B alloys [22, 23]. Additionally, Al_2O_3 particles which were retained from the pack cementation process are occasionally embedded within the borosilicate layer.

However, since the substrate is a Ti-containing Mo-Si-B alloy, some TiO_2 forms during the pack cementation and conditioning. The TiO_2 is located at the surface with a plate-like shape as well as in form of particulates within the borosilicate layer. A typical micrograph of the coated surface is shown in Fig. 2 c). Here, cavities within the borosilicate are frequently found as defects of the surface coating. In addition to the outer borosilicate layer, the coating consists of different silicide layers after conditioning. The identification of the layer sequence is based on both, local chemical (EDX) as well as local structural characterization (EBSD) as can be seen in Fig. 2 d. The sequence from the borosilicate to the substrate is (i) $MoSi_2$ (space group 139, a = 3.21 Å, c = 7.58 Å) with particles that are probably the MoB phase [23], (ii) a Ti_5Si_3 layer (space group 193, a = 7.46 Å, c = 5.13 Å) with $MoSi_2$/Mo_5Si_3 (space group 140, a = 9.65 Å, c = 4.91 Å) particles. The $MoSi_2$ particles within the Ti_5Si_3 are close to the $MoSi_2$ layer, while the Mo_5Si_3 particles are adjacent to the substrate. Additionally, the boundary between Ti_5Si_3 and the substrate has a higher volume fraction of Mo_3Si compared to the substrate. It has to be noted that the $MoSi_2$ and the Ti_5Si_3 phase are not in equilibrium with each other. It can be assumed that the sluggish diffusion within Mo is prohibiting the equilibrium condition [24, 25]. Fig. 2 b) shows a pore within the silicide layers, which is connected to the borosilicate layer by a crack, too. Cracking in the coating structure was also observed in literature for Si pack cementation on Mo-Si-B alloys [22, 23]. It is noteworthy, that those cracks are filled easily by the borosilicate glass layer resulting in a self-healing effect.

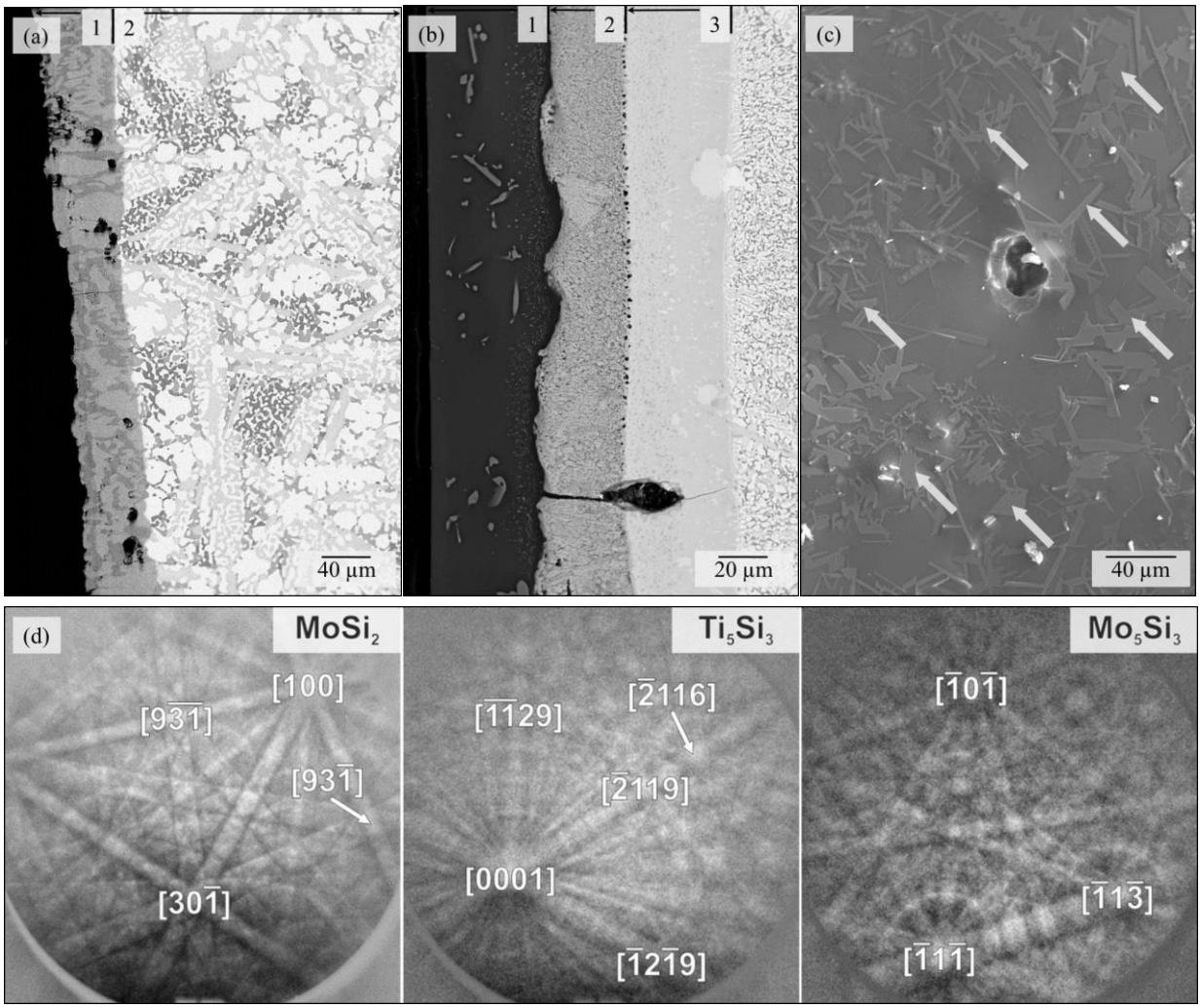

FIG. 2. SEM micrographs showing a) 1 pack cementation coating and 2 substrate material (bright – Mo_{ss}, grey – Mo_5SiB_2, dark – Ti_5Si_3), b) the resulting layer structure (1 is a borosilicate layer with embedded TiO_2 and Al_2O_3 particles, 2 is a $MoSi_2$ layer with probably MoB [23] and 3 is a Ti_5Si_3 layer having $MoSi_2$ and Mo_5Si_3 particles embedded), c) the layer surface (TiO_2 indicated by arrows and a cavity in the center) after conditioning at 1400 °C for 10 h, d) selected electron backscatter diffraction patterns with according zone axes for phase identification.

Since the exposure of borosilica to high temperature is known to promote boron loss [28, 29] EPMA measurements were conducted to determine the boron content in the coating on a Mo sample (without Ti) after pack cementation with a Si/B ratio of 35/1 and conditioning at 1400 °C for 25 h. This is a longer conditioning treatment than that used for the Mo-Si-B-Ti alloys. The results are given in Table 3 and clearly reveal that there is retention of boron at a level close to that in the initial pack content. The retention is attributed to the presence of both Al and Na in the coating that are incorporated during the pack cementation process and have been shown to suppress the loss of boron in borosilica [30, 31]. The measured boron content is sufficient to reduce the viscosity of silica by about two orders of magnitude [32]. Moreover, the boron level in the T_1 phase will act as a reservoir to maintain the boron in the coating.

Table 3. Composition Measurements for the coating and Mo_5Si_3 (T_1) phase

Orientation	B at.%	Al at.%	Na at.%	Mo at.%	O at.%	Si at.%	at.% Totals
Coating Cross-section	0.96	3.20	0.01	0.45	66.52	28.85	100
Cross-section T_1	4.03	0.02	0.02	61.77	6.62	27.54	100

Oxidation Behavior

The isothermal oxidation weight changes for 1100 and 1200 °C are summarized in Fig. 3 a). The samples oxidized at 1200 °C show a negligible weight change throughout the 100 h exposure. At 1100 °C one sample exhibited the same behavior as that observed at 1200 °C. However, the second sample showed a mass loss until it reached a steady state after 50 h of oxidation. The reason for the initial mass loss is most likely due to formation of MoO_3, which evaporates at possible defects in the borosilicate layer as indicated in Fig. 2 c). Since the weight change curves reach steady state, it can be assumed that even by incomplete covering of the borosilicate layer after pack cementation and conditioning, the coating is able to passivate and cover such defects. The analysis of the cross-sections of the isothermal oxidized samples show no change in the layer morphology compared to the as conditioned stage.

The long term oxidation behavior of the applied borosilicate layer was studied under thermal cycling conditions, which are known to be more crucial for materials in technical applications compared to isothermal oxidation, because spallation is promoted. Spallation can be caused by either poor adhesion between the substrate and the coating or by different thermal expansion coefficients of the substrate and the coating, resulting in interfacial stress during cooling and heating [14].

The weight change curves of the cyclic oxidation tests for each test temperature are summarized in Fig. 3 b). For the sake of clarity, a scale break from 550 to 850 h is applied to the time axis. At 800 °C, all samples show an initial weight loss around 3 to 4 mg/cm² followed by a steady state with no further distinct weight change. With increasing temperature, the weight loss becomes less for 1100 °C and turns into a weight gain at 1200 °C. However, at higher temperatures the weight change is more variable compared to 800 °C. One of the samples oxidized at 1100 °C has a larger weight loss than the others and at 1200 °C one of the three samples reached a steady state, while the other two show a mass gain over time. A better overview of the initial states of oxidation is represented in Fig. 3 c), where the specific weight change for the first 25 h of cyclic oxidation is plotted. The majority of mass loss at 800 °C occurs within the first 10 h of oxidation. At the same time the oxidation behavior at 1100 °C turns from mass loss to mass gain, whereas this point is reached after approximately 5 h at 1200 °C. As for the isothermal oxidation tests, the initial weight loss is assumed to be a result of an incomplete conditioning by the formation of cracks within the borosilicate layer during cooling or by incomplete covering of the samples surface. The initial weight loss at 800 °C during thermal cycling (Fig. 3 b, c) for the coated sample is rather minimal compared to the uncoated sample (Fig. 3 d) as indicated by the weight change scales in Fig. 3. The initial loss is related to the increased time during heating to a low temperature (i.e. 800 °C) for the coating to flow and cover defects (Fig. 2 c) and cracks that develop in the $MoSi_2$ layer (Fig. 2 b) during cooling. The faster turnover from mass loss to mass gain at 1200 °C in contrast to 1100 °C is caused by the lower viscosity of the borosilicate glass at higher temperatures [13, 26].

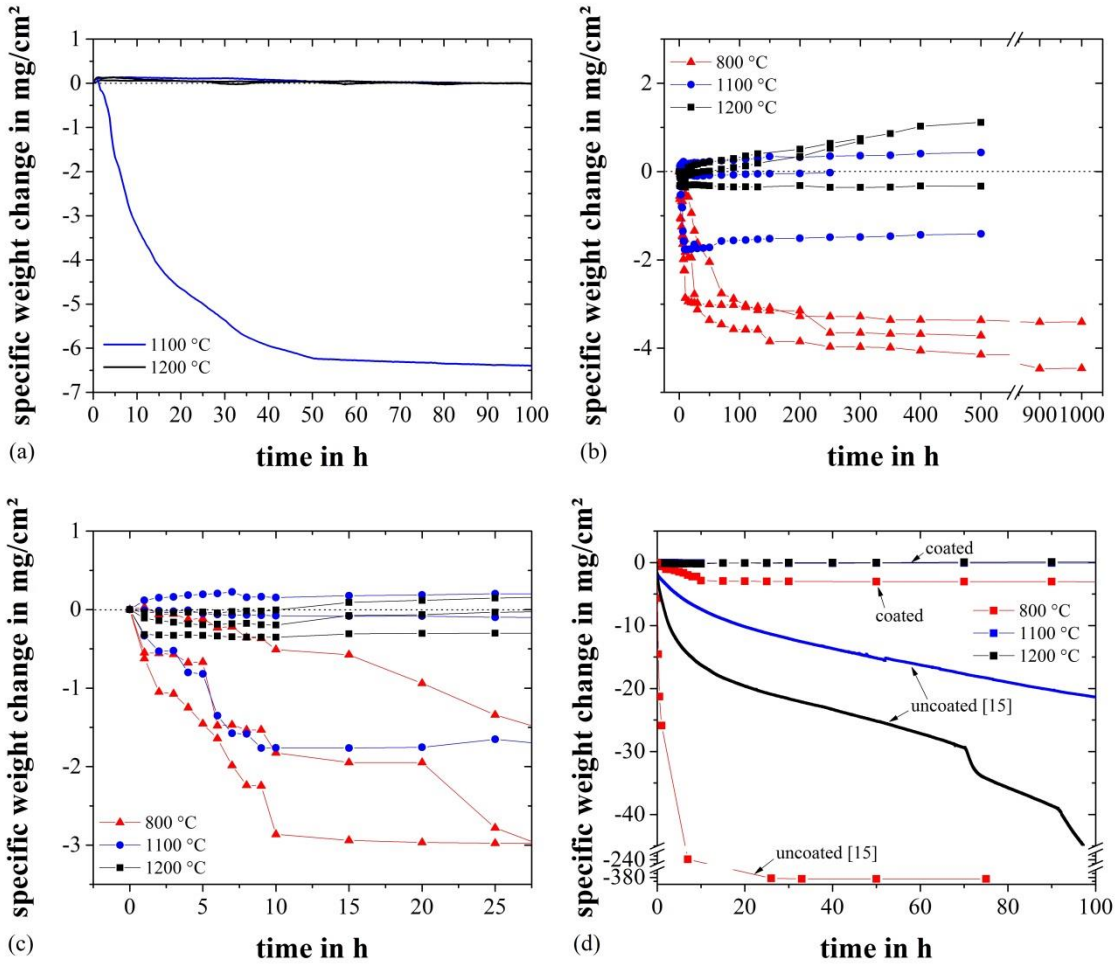

FIG. 3. Weight change vs. time for coated Mo-12.5Si-8.5B-27.5Ti at a) isothermal conditions at 1100 and 1200 °C, b) thermal cycling at 800, 1100 and 1200 °C, c) the initial stage of b) and d) the comparison with literature data of [15].

Fig. 3 d) summarizes the weight change curves for the thermal cycling and provides a comparison with the weight change behavior of uncoated Mo-12.5Si-8.5B-27.5Ti investigated by Azim et al. [15] at the same oxidation temperatures. While the weight change at 1100 and 1200 °C is negligible for the coating, the weight change for the uncoated alloy is 22 and 43 mg/cm² after 100 h of oxidation without reaching steady state. However, at 800 °C the uncoated substrate is fully consumed by the oxidation process within the first 20 h of oxidation, while the weight loss for the coated substrate is about 2 mg/cm² at the same time. The main reason for the improved oxidation resistance is the suppressed formation of TiO_2 during oxidation by the $MoSi_2$ layer, which acts as a diffusion barrier for Ti due to negligible solubility of Ti in $MoSi_2$ [27]. The determined oxidation behavior of the coated Mo-Si-B-Ti alloy is consistent to the observed behavior of Ti-free Mo-Si-B alloys coated by Al pack cementation [20, 23].

The thickness of the separate layers was determined by image processing program for all oxidation temperatures after 500 h of oxidation and is compared with the as conditioned layers in Fig 4. For all oxidation temperatures the layer thickness remains stable, even if the borosilicate layer at 1200 °C is slightly smaller. This is assumed to be a result of the lower Al_2O_3 content within the coating, that leads to a lower standard deviation (the error bars in Fig 4). At 1100 °C for example the Al_2O_3 content was much higher, resulting in larger layer thickness and higher standard deviation. Furthermore, the growth of the borosilicate layer is assumed to result in the measured weight gain, even if the determined very small weight change does not lead to a significant change in layer thickness. For a starting sample thickness of 4.46 mm, the sample thickness after exposure at 1200 °C for 500 h decreased by about 60 µm. This represents a decrease of about 1.3% that is shared between the top and bottom of the sample. Some of this change is due to the conversion of the Mo phase into $MoSi_2$. Thus, the substrate recession is minimal.

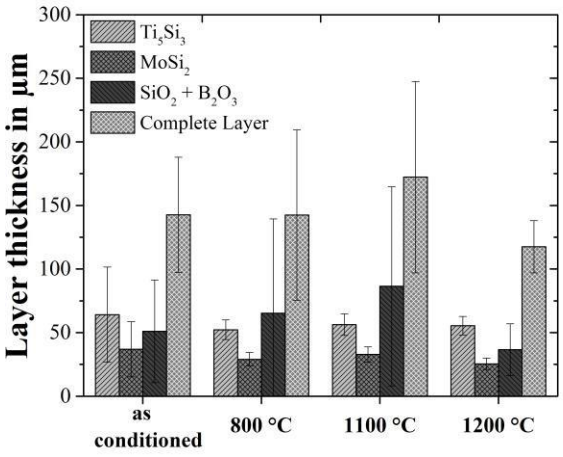

FIG. 4. Comparison of layer thickness between conditioning stage at 1400 °C for 10 h and after thermal cycling at 800, 1100 and 1200 °C for 500 h.

CONCLUSIONS

By co-deposition of (Si+B) during pack cementation followed by a high temperature conditioning treatment, a borosilicate based coating has been established on a model Mo-Si-B-Ti alloy. In addition to the representative coating layers of an outer borosilicate glass and inner $MoSi_2$ and Ti_5Si_3 layers, some TiO_2 develops either as surface plate shaped particles or as isolated particles within the glass. The substrate microstructure is unaltered by the coating process. During both isothermal and cyclic oxidation after an initial mass loss of about 4 mg/cm² during the first hours of exposure, a steady state is reached for times up to 1000 h at temperatures ranging from 800 to 1200 °C demonstrating a significantly enhanced oxidation resistance. The effectiveness of the coating is not diminished by the presence of isolated TiO_2 particles. Furthermore, the coating appears to exhibit a self-healing capability to damage such as cracking in the $MoSi_2$ layer due to the formation of the borosilicate glass.

ACKNOWLEDGMENTS

The financial support of Deutsche Forschungsgemeinschaft (DFG) and by Karlsruhe House of Young Scientists (KYHS) is gratefully acknowledged. AK thanks the Carl Zeiss Foundation for funding. The support of ONR (N00014-10-1-0913) for JHP is gratefully acknowledged. This work was partly carried out with the support of the Karlsruhe Nano Micro Facility (KNMF, www.knmf.kit.edu), a Helmholtz Research Infrastructure at Karlsruhe Institute of Technology (KIT, http://www.kit.edu).

REFERENCES

[1] B. P. Bewlay, M. R. Jackson and H. A. Lipsitt, *Metall. Mater. Trans. A* **27,** 3801 (1996).
[2] P. Jéhanno, M. Heilmaier, H. Saage, M. Böning, H. Kestler, J. Freudenberger and S. Drawin, *Metall. Mater. Trans. A* **36A**, (2005).
[3] J. H. Perepezko, *Science* **326**, 5956 (2009).
[4] P. Jain and K. S. Kumar, *Acta Mater.* **58**, 2124 (2010).
[5] S. Burk, B. Gorr, V. B. Trindade and H.-J. Christ, *Oxid. Met.***73**, 163 (2009).
[6] J. H. Schneibel, *Intermetallics* **11**, 625 (2003).
[7] S. Burk, B. Gorr, V. B. Trindade, U. Krupp, und H.-J. Christ, , *Corros. Eng. Sci. Technol.*, Bd. 44, Nr. 3, S.

168–175, Juni 2009.
[8] G. Erickson, „A new, third-generation, single-crystal, casting superalloy“, *JOM J. Miner. Met. Mater. Soc.* **47,** 36 (1995).
[9] M. Krüger, S. Franz, H. Saage, M. Heilmaier, J. H. Schneibel, P. Jéhanno, M. Böning and H. Kestler, *Intermetallics* **16**, 933 (2008).
[10] J. J. Kruzic, J. H. Schneibel and R. O. Ritchie, *Scr. Mater.* **50**, 459 (2004).
[11] J. H. Schneibel, M. J. Kramer, Ö. Ünal and R. N. Wright, *Intermetallics* **9**, 25 (2001).
[12] M. Krüger, D. Schliephake, P. Jain, K. S. Kumar, G. Schumacher and M. Heilmaier, *JOM* **65**, 301 (2012).
[13] T. Parthasarathy, M. Mendiratta and D. Dimiduk, *Acta Mater.* **50**, 1857 (2002).
[14] D. Schliephake, M. Azim, K. von Klinski-Wetzel, B. Gorr, H.-J. Christ, H. Bei, E. P. George and M. Heilmaier, *Metall. Mater. Trans. A* **45**, 1 (2013).
[15] M. A. Azim, D. Schliephake, C. Hochmuth, B. Gorr, H.-J. Christ, U. Glatzel and M. Heilmaier, *JOM* **67**, 2621 (2015).
[16] M. Azim, S. Burk, B. Gorr, H.-J. Christ, D. Schliephake, M. Heilmaier, R. Bornemann and P. Haring Bolivar, *Oxidation of Metals* **80**, 231 (2013).
[17] Y. Yang, H. Bei, S. Chen, E. P. George, J. Tiley and Y. A. Chang, *Acta Mater.* **58**, 541 (2010).
[18] S. Burk, B. Gorr, H.-J. Christ, D. Schliephake, M. Heilmaier, C. Hochmuth and U. Glatzel, *Scr. Mater.***66**, 223 (2012).
[19] B. A. Pint, J. R. DiStefano and I. G. Wright, *Mater. Sci. Eng. A* **415**, 255 (2006).
[20] R. Sakidja, F. Rioult, J. Werner and J. H. Perepezko, *Scr. Mater.* **55**, 903 (2006).
[21] J. S. Park, R. Sakidja and J. H. Perepezko, *Scr. Mater.* **46**, 765 (2002).
[22] R. Sakidja, J. S. Park, J. Hamann and J. H. Perepezko, *Scr. Mater.* **53**, 723 (2005).
[23] J. H. Perepezko and R. Sakidja, *JOM*, **62**,13 (2010).
[24] K. Meier, H. Mehrer and R. Gerhard, *Z. für Met.***70**, 271 (1979).
[25] R. Sakidja, H. Sieber and J. H. Perepezko, *Philos. Mag. Lett.*,**79**, 351 (1999).
[26] D. M. Dimiduk and J. H. Perepezko, *MRS Bull.*, **28**, 639 (2003).
[27] P. S. Frankwicz and J. H. Perepezko, in *Symposium Q – High-Temperature Ordered Intermetallic Alloys IV*, 1990, MRS **213**, p. 169.
[28] M. Singh and H. Wiedemeier, J. Am. Ceram. Soc., **74**, 724 (1991).
[29] P. Meschter, E. Opila and N.S. Jacobson, Ann. Rev. Mater. Res., **43**, 559 (2013).
[30] K. Grente, F. Rebillat and F. Langlais, High Temp. Corrosion and Mater. Chem. IV Book Series: Electrochem. Soc. Series**, volume 2003**, issue 16, 545 (2003).
[31] R.H. Doremus, Am. Ceram. Soc. Bull., **82**, (3) 59 (2003).
[32] N.P. Bansal and R.H. Doremus, eds.," Handbook of Glass Properties", Academic Press Orlando, FL,(1919).